A Letters Journal Exploring the Frontiers of Physics

February 2020

EPL, **129** (2020) 42001 www.epljournal.org
doi: 10.1209/0295-5075/129/42001

# Coherent J/$\psi$ photoproduction in peripheral heavy-ion collisions

O. Bugnon for the ALICE Collaboration

*SUBATECH, IMT Atlantique, Université de Nantes, CNRS-IN2P3 - Nantes, France*

received 23 October 2019; accepted in final form 4 March 2020
published online 30 March 2020

PACS 25.20.Lj – Photoproduction reactions
PACS 14.40.Pq – Heavy quarkonia
PACS 24.85.+p – Quarks, gluons, and QCD in nuclear reactions

**Abstract** – In 2015, the ALICE Collaboration reported the first measurement of an excess in the yield of J/$\psi$ at very low transverse momentum ($p_{\mathrm{T}} < 0.3\,\mathrm{GeV}/c$) in the forward rapidity region ($2.5 < y < 4$) in peripheral lead-lead (Pb-Pb) collisions at $\sqrt{s_{\mathrm{NN}}} = 2.76\,\mathrm{TeV}$ at the CERN LHC. The coherent photoproduction was proposed as the potential underlying physics mechanism. This is known to be the main production mechanism for low-$p_{\mathrm{T}}$ J/$\psi$ production in ultra-peripheral collisions, which are dominated by electromagnetic interactions. However, the observation of a large effect in more central collisions that are dominated by the hadronic interactions was quite surprising. This article represents a proceeding contribution on the preliminary results from Pb-Pb collisions at $\sqrt{s_{\mathrm{NN}}} = 5.02\,\mathrm{TeV}$ shown in a poster during the National Congress of the French Physical Society in July 2019.



**Introduction.** – Experiments with ultra-relativistic heavy-ion collisions (HIC) aim at studying the hadronic matter at high temperature and energy density. According to Quantum Chromodynamics (QCD), a deconfined state of partonic matter, the Quark-Gluon Plasma (QGP), is expected to be formed in collisions of heavy ions at energies available at the CERN Large Hadron Collider (LHC) and the BNL Relativistic Heavy Ion Collider (RHIC).

Heavy quarks are expected to be produced at the early stages of the collision and, therefore, they experience the whole hot QCD medium evolution. The formation of charm and anti-charm ($c\bar{c}$) bound states, known as charmonia, whose vector state with lower mass is the J/$\psi$, is expected to be affected by the interaction with the strongly interacting medium. In presence of a QGP, a color-charge screening mechanism is expected to prevent the formation of the charmonium states. With the increase of the medium temperature, the screening effect becomes stronger, preventing the formation of tightly bound states. Thus, the sequential suppression of charmonium states was suggested to be used as a temperature probe for the QGP [1]. However, other mechanisms affect the charmonium production in presence of the QGP. In particular, the J/$\psi$ can be regenerated during or at the end of the deconfined phase due to the recombination of initially uncorrelated $c$ and $\bar{c}$ quarks [2,3]. The recombination probability is expected to increase with the charm density and thus with the collision energy and the centrality of the collision. Lastly, effects related to the initial state of the partons in the nuclei but unrelated to the QGP formation, the cold nuclear matter effects, significantly affect the charmonium production in heavy-ion collisions and must be taken into account when studying the medium properties [4,5].

The J/$\psi$ production in Pb-Pb collisions has been extensively studied by the ALICE Collaboration at a center-of-mass energy of $\sqrt{s_{\mathrm{NN}}} = 2.76\,\mathrm{TeV}$ and $\sqrt{s_{\mathrm{NN}}} = 5.02\,\mathrm{TeV}$ [6–8]. Nuclear effects are usually quantified via the so-called nuclear modification factor ($R_{\mathrm{AA}}$) which is the ratio of the J/$\psi$ yield in Pb-Pb collisions divided by its production cross section in pp collisions at the same collision energy scaled by the nuclear overlap function that accounts for the number of binary nucleon-nucleon collisions in a nucleus-nucleus collision.

ALICE reported a very large value of the J/$\psi$ $R_{\mathrm{AA}}$ at very low $p_{\mathrm{T}}$ (*i.e.*, $p_{\mathrm{T}} < 0.3\,\mathrm{GeV}/c$) in peripheral Pb-Pb collisions at $\sqrt{s_{\mathrm{NN}}} = 2.76\,\mathrm{TeV}$ that could not be reproduced by theoretical calculations involving hadroproduction mechanisms alone [9,10]. This observation was confirmed by the STAR Collaboration in Au-Au and U-U collisions at lower energies [11]. Coherent photoproduction of vector mesons was suggested as the underlying physics mechanism. In this process, a quasi-real photon produced coherently by the electromagnetic field of one nucleus interacts coherently with the gluon field of the other to produce a vector meson. This process is well known thanks to various studies at the electron-proton (e-p) collider HERA at DESY [12] and in nucleus-nucleus (A-A) Ultra-Peripheral Collisions (UPC) at the LHC [13–15] and RHIC [16,17] and it allows probing the gluonic content of nuclei. However, the observation of such a process was unexpected in peripheral collisions and it opens questions on the coherent condition in hadronic collisions despite the nuclear overlap. Throughout this paper, the term coherent is used to describe the interaction, in analogy with UPC, although in this case it is not clear how the coherence arises in a system where the nuclei eventually break up.

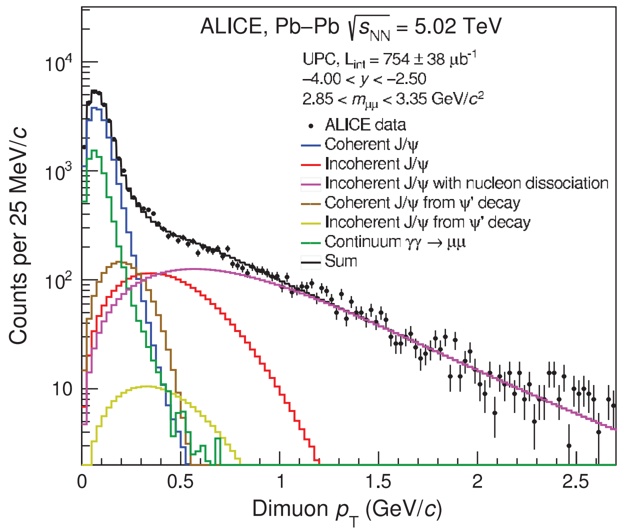


Fig. 1: Transverse momentum distribution of opposite-sign dimuon pairs for $2.85 < m_{\mu\mu} < 3.35\,\mathrm{GeV}/c^2$ and $-4 < y < -2.5$ in UPC Pb-Pb at $\sqrt{s_{\rm NN}} = 5.02\,\mathrm{TeV}$ [15].

**Photoproduction of J/$\psi$ mesons in UPC with ALICE.** – A detailed review of the UPC physics at the LHC can be found in [18]. These collisions are characterized by an impact parameter larger than the sum of the radii of the incoming nuclei ($b > R_1 + R_2$) and correspond to photon-induced processes without hadronic interactions. The intense electromagnetic field of one nucleus acts as a source of virtual photons with a flux proportional to the square of the charge of the nucleus ($Z$) and to the charge distribution of the nucleus described by the nuclear form factor ($F$) [19]. This flux is described by the Weizsäcker-Williams quasi-real photon approximation [20,21]. Photons may fluctuate into $q\bar{q}$ pairs that will scatter off the other nucleus to emerge as a vector meson. At leading order (LO) in perturbative QCD (pQCD), the process implies the exchange of two gluons in a singlet color state. The corresponding photonuclear cross section should be proportional to the square of the nuclear gluon distribution function (nPDF) at a given value of Bjorken-$x$ with $x(\pm y) = (m_{\mathrm{J}/\psi}/\sqrt{s_{\rm NN}})\exp(\pm y)$, $m_{\mathrm{J}/\psi}$ being the J/$\psi$ mass and $y$ the rapidity. The J/$\psi$ coherent photoproduction cross section at a given rapidity $y$ can be expressed as the product of the photon flux $n_\gamma(\pm y, \{b\})$ and the photo-nuclear cross section $\sigma_{\gamma\mathrm{A}}(\pm y)$, where $\{b\}$ is the impact parameter range. In A-A collisions, this process is the sum of two contributions. They correspond to the configuration where the ion moving towards (away from) the detector emits a high- (low-) energy photon and scatters off the other ion probing the gluonic content at low- (high-) $x$ values. At LHC energies, the probed Bjorken-$x$ values range from $x(-y) \sim 10^{-5}$ to $x(+y) \sim 10^{-2}$. Therefore, UPC provide a valuable tool to investigate nuclear modification effects on the gluon PDFs such as the gluon shadowing [22].

The coherence condition in heavy vector meson photoproduction imposes an average transverse momentum $\langle p_{\rm T}\rangle$ of the order of $1/R_{\rm nucleus}$. One can distinguish between the coherent and the incoherent photoproduction of vector mesons [15]. In the first case, the photon interacts with the gluon field of the entire nucleus target. This leads to a low transverse momentum J/$\psi$ ($\langle p_{\rm T}\rangle \simeq 60\,\mathrm{MeV}/c$) and no breaking-up of the target nucleus. In the second case, the photon couples to a single nucleon, implying that the produced J/$\psi$ has a larger $p_{\rm T}$ ($\langle p_{\rm T}\rangle \simeq 500\,\mathrm{MeV}/c$) and the target nucleus usually breaks up.

The photoproduction of J/$\psi$ is studied in ALICE in Pb-Pb UPC via their dimuon decay channel. Figure 1 shows the latest results of the $p_{\rm T}$ distribution of opposite-sign dimuons in ultra-peripheral Pb-Pb collisions at $\sqrt{s_{\rm NN}} = 5.02\,\mathrm{TeV}$. Besides the coherent and incoherent photoproduction, low-$p_{\rm T}$ J/$\psi$ can be produced by the decay of $\psi$(2S), a higher mass charmonium state, that could be created by coherent and incoherent photoproduction. Finally, the electromagnetic continuum process $\gamma\gamma \to \mu^+\mu^-$ contributes to low-$p_{\rm T}$ dimuons as the main background source in UPC which is subtracted using the fit to the dimuon invariant mass distribution. These results provide input for the analysis in peripheral events, see eq. (2).

**ALICE experiment.** – The ALICE detector and its performance are described in [23] and [24], respectively. At forward rapidity ($2.5 < y < 4$), the charmonia are reconstructed in their dimuon decay channel with the muon spectrometer. It consists of a front absorber of composite material to reduce hadron contamination, five tracking stations, the third of which is placed inside a dipole magnet that provides a $3\,\mathrm{T}\cdot\mathrm{m}$ magnetic field integral, followed by an iron wall and two trigger stations. The muon spectrometer was specially designed to study charmonium and vector meson production in their dimuon decay channel down to zero $p_{\rm T}$. Three other detectors are used in this analysis. The Silicon Pixel Detector (SPD), the inner part of the Silicon Tracker Detector placed at midrapidity, provides the coordinates of the primary interaction vertex. The V0 detector, consisting of two arrays of scintillator tiles placed on both sides of the interaction point at forward rapidities, is used to reject beam-gas interaction background and to measure the centrality of the collision and the luminosity. The centrality determination is based on a Glauber model fit to the signal amplitude in the V0 detectors. The centrality is expressed as a percentile of the total nuclear interaction cross section. The V0 also provides a minimum bias (MB) trigger, defined by the coincidence of a signal in the two V0 arrays. Finally the Zero Degree Calorimeters (ZDC) placed at forward rapidities, are used to reject the electromagnetic background.

The presented analysis exploits the data samples of Pb-Pb collisions at $\sqrt{s_{\rm NN}} = 5.02\,\text{TeV}$ collected in 2015. A dimuon trigger is applied, requiring a coincidence between a MB trigger and the presence in the muon trigger chambers of two opposite-sign muons, each with a $p_{\rm T}$ above a threshold of $1\,\text{GeV}/c$. The data sample corresponds to an integrated luminosity $\mathcal{L}_{\rm int} \approx 225\,\mu\text{b}^{-1}$ in the dimuon decay channel. The analysis focuses on the most peripheral events, *i.e.*, the centrality ranges 50–70% and 70–90%.

**Data analysis.** – Figure 2 shows the raw $p_{\rm T}$ distribution of opposite-sign dimuons at forward rapidity in the J/$\psi$ mass range $2.8 < m_{\mu\mu} < 3.4\,\text{GeV}/c^2$, for the most peripheral events, *i.e.*, centrality range 70–90%. A significant excess is observed at very low $p_{\rm T}$ ($p_{\rm T} < 200\,\text{MeV}/c$) with a shape similar to the one reported in UPC (fig. 1).

The J/$\psi$ candidates are extracted by fitting the dimuon invariant mass distribution obtained by combining all pairs of opposite-sign muons in the geometrical acceptance of the muon spectrometer that match a tracklet in the trigger system passing the trigger $p_{\rm T}$ condition. In addition, the $p_{\rm T}$ of the pair is required to be smaller than $0.3\,\text{GeV}/c$. Figure 3 shows the signal extraction for the most peripheral centrality class (70–90%). The signal is described by a function with a Gaussian core and power-law tails that take into account different detector effects. The background contribution in the invariant mass range $2.8 < m_{\mu\mu} < 3.4\,\text{GeV}/c^2$ is negligible.

The raw J/$\psi$ excess measurement with respect to the hadronic contribution requires to quantify the latter and subtract it from the raw number obtained in the signal extraction. The number of J/$\psi$ from hadroproduction is estimated as

$$\frac{\mathrm{d}N_{\rm AA}^{\rm h\ J/\psi}}{\mathrm{d}p_{\rm T}} = \mathcal{N} \times \frac{\mathrm{d}\sigma_{\rm pp}^{\rm h\ J/\psi}}{\mathrm{d}p_{\rm T}} \times R_{\rm AA}^{\rm h\ J/\psi} \times (\mathcal{A}\times\epsilon)_{\rm AA}^{\rm h\ J/\psi}, \qquad (1)$$

where $\mathrm{d}\sigma_{\rm pp}^{\rm h\ J/\psi}/\mathrm{d}p_{\rm T}$ is the J/$\psi$ hadronic cross section in pp collisions at 5.02 TeV [25], $R_{\rm AA}^{\rm h}$ is the nuclear modification factor of hadronic J/$\psi$ in Pb-Pb collisions at 5.02 TeV [8], $(\mathcal{A}\times\epsilon)_{\rm AA}^{\rm h}$ is the hadronic J/$\psi$ acceptance times efficiency

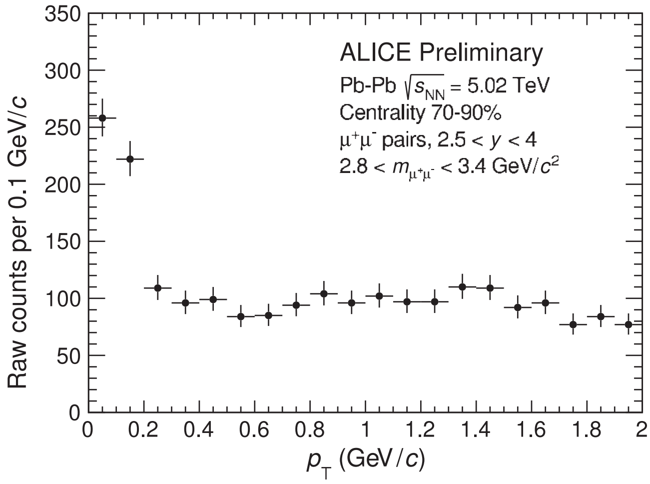


Fig. 2: $p_{\rm T}$ distribution of opposite-sign dimuons for $2.8 < m_{\mu\mu} < 3.4\,\text{GeV}/c^2$ and $2.5 < y < 4$ in peripheral Pb-Pb collisions at $\sqrt{s_{\rm NN}} = 5.02\,\text{TeV}$.

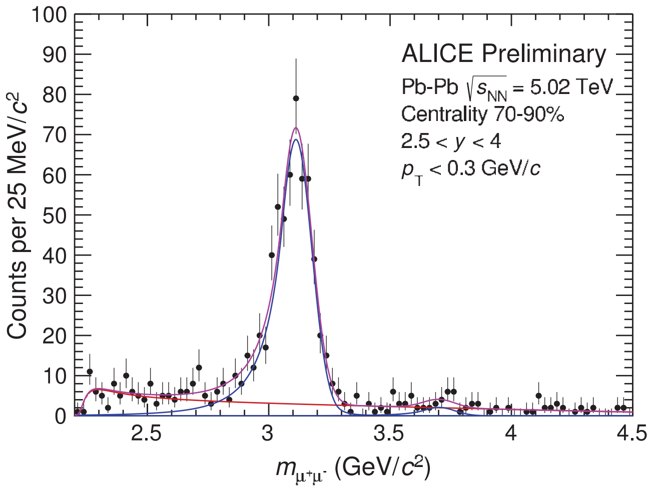


Fig. 3: Invariant mass distribution of opposite-sign dimuons for $p_{\rm T} < 0.3\,\text{GeV}/c$ and $2.5 < y < 4$ in peripheral Pb-Pb collisions at $\sqrt{s_{\rm NN}} = 5.02\,\text{TeV}$.

obtained by a Monte Carlo simulation, and $\mathcal{N}$ the normalization factor fixed in a such a way that the number of J/$\psi$ obtained by integrating eq. (1) in the $p_{\rm T}$ interval 1–8 GeV/$c$ where the hadroproduction is dominant, is equal to the measured one.

Finally, the number of coherently photoproduced J/$\psi$ is obtained by correcting the raw J/$\psi$ excess ($N^{\rm exc\ J/\psi}$) by the fraction of incoherently photoproduced J/$\psi$ ($f_{\rm I}$) and the fraction of J/$\psi$ from the decay of coherently photoproduced $\psi$(2S) ($f_{\rm D}$). The fractions $f_{\rm I}$ and $f_{\rm D}$ used in this anaysis are obtained from the results of J/$\psi$ photoproduction in Pb-Pb UPC at 2.76 TeV [13] with the assumption that they are energy independent. This assumption represents the main source of systematic uertainties in this analysis. The yield of coherent photoproduced J/$\psi$ is defined as

$$Y^{\mathrm{coh}\ J/\psi} = \frac{\frac{N^{\mathrm{exc}\ J/\psi}}{1+f_{\mathrm{I}}+f_{\mathrm{D}}}}{B.R. \times (\mathcal{A} \times \epsilon)^{\mathrm{coh}} \times N_{\mathrm{MB}}}, \tag{2}$$

where $B.R. = 5.93\%$ is the branching ratio of the J/$\psi$ decaying to dimuons, $N_{\mathrm{MB}}$ is the number of MB events corresponding to the analysed number of dimuon-triggered events and $(\mathcal{A} \times \epsilon)^{\mathrm{coh}}$ is the acceptance times efficiency for the coherent J/$\psi$ photoproduction obtained using MC simulations. The difference between $\mathcal{A}^{\mathrm{h}}$ and $\mathcal{A}^{\mathrm{coh}}$ is due to the fact that, in the MC simulation, photoproduced J/$\psi$ are assumed to be transversally polarized as expected [26,27]. The coherent J/$\psi$ photoproduction cross section at $\sqrt{s_{\mathrm{NN}}} = 5.02$ TeV is finally evaluated starting from the corresponding cross section at $\sqrt{s_{\mathrm{NN}}} = 2.76$ TeV [9], normalized by the ratio of the yields at the two energies. This ratio shows an increase with energy by a factor $2.62 \pm 0.42$ (stat.) $\pm\, 0.18$ (syst.) ($3.52 \pm 1.02$ (stat.) $\pm\, 0.42$ (syst.)) in the centrality class 70–90% (50–70%), showing no strong centrality dependence within uncertainties. The systematic uncertainty on the cross section is the quadratic sum of the uncertainties from different sources. The main sources of uncertainty on this analysis are the description of the J/$\psi$ invariant mass distribution on the signal extraction, the MC input used in the $(\mathcal{A} \times \epsilon)$ estimation and the evaluation and the energy dependence of the fractions $f_{\mathrm{I}}$ and $f_{\mathrm{D}}$. The first source is estimated by using several modelizations for the tails of the distribution in the fit. The second is estimated by making two extreme assumption on the polarisation of the J/$\psi$ (namely fully polarised or no polarisation). The last one is estimated by considering a conservative 100% systematic uncertainty on $(f_{\mathrm{I}} + f_{\mathrm{D}})$.

**Results.** – Figure 4 shows the preliminary results on the coherent J/$\psi$ photoproduction cross section at forward rapidity in the dimuon channel together with similar preliminary results at midrapidity in the dielectron channel for the centrality class 50–70% at $\sqrt{s_{\mathrm{NN}}} = 5.02$ TeV. Figure 5 shows the results in the same rapidity intervals for the centrality class 70–90%. The results are compared with theoretical models. The Golec-Biernat-Wusthoff (GBW) model is a light-cone color dipole formalism and the Iancu-Itakura-Munier (IIM) model is another dipole formalism based on the Color Glass Condensate approach of [28]. The GG-hs and GS-hs calculations are two energy-dependent hot-spot models [29] using the Glauber-Gribov formalism and geometric scaling, respectively. All models implement a modification of the photon flux in peripheral collisions compared to the ultraperipheral case. In addition, both dipole models include partonic saturation effects and nuclear shadowing effects as well as an effective photonuclear cross section whereas the hot-spot models are an extrapolation from photon-proton to photon-lead interactions. All models can qualitatively reproduce the data in both rapidity regions, with a tendency to overestimate the data at midrapidity for the centrality class

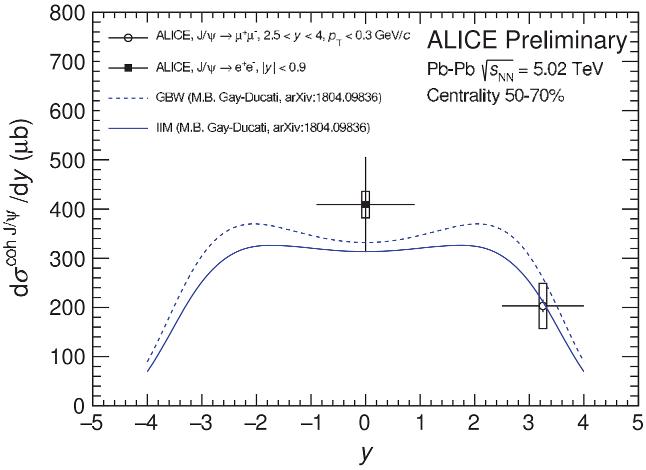


Fig. 4: Cross section for the J/$\psi$ coherent photoproduction at forward and midrapidity in Pb-Pb collisions at $\sqrt{s_{\mathrm{NN}}} = 5.02$ TeV in the centrality class 50–70%. The results are compared with theoretical calculations from [28].

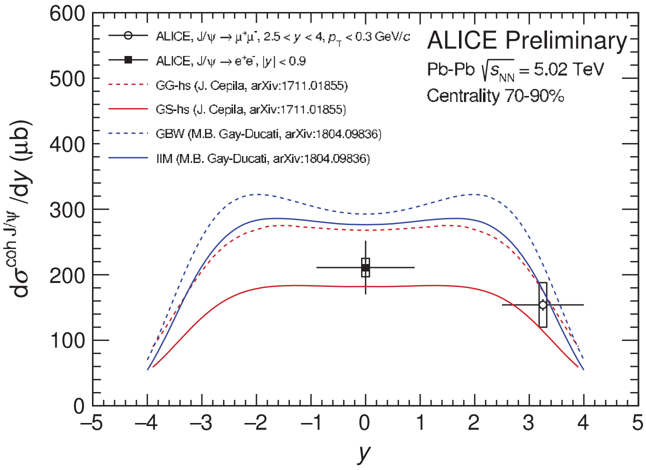


Fig. 5: Cross section for the J/$\psi$ coherent photoproduction at forward and midrapidity in Pb-Pb collisions at $\sqrt{s_{\mathrm{NN}}} = 5.02$ TeV in the centrality class 70–90%. The results are compared with theoretical calculations from [28] and [29].

70–90%. A better experimental precision would be helpful for a sharper conclusion.

**Discussion.** – The excess in the yield of J/$\psi$ at very low $p_{\mathrm{T}}$ was confirmed in peripheral events at mid- and forward rapidity in Pb-Pb collisions at $\sqrt{s_{\mathrm{NN}}} = 5.02$ TeV with an increase of the yield of coherently photoproduced J/$\psi$ by up to a factor $\sim 3$ with respect to $\sqrt{s_{\mathrm{NN}}} = 2.76$ TeV. Theoretical models of coherent J/$\psi$ photoproduction are able to describe the measured cross section results for both rapidity ranges within uncertainties. The precision of the measurement will be improved thanks to the new and larger data sample of Pb-Pb collisions at $\sqrt{s_{\mathrm{NN}}} = 5.02$ TeV collected in 2018 and to the new values of $f_{\mathrm{I}}$ and $f_{\mathrm{D}}$ from Pb-Pb UPC at the same energy [15]. With a large enough data sample, the measurement of a rapidity differential cross section will help to constrain and discriminate between different models. In addition, the study will be extended to more central collisions to test the centrality dependence of the $p_{\mathrm{T}}$ distribution where two extreme hypotheses can be tested. In the first, all nucleons in the target ion participate to the photonuclear cross section despite the nuclear overlap, resulting in no centrality dependence of the J/$\psi$ $\langle p_{\mathrm{T}} \rangle$. The second hypothesis favours a scenario in which only spectators participate to the process. In such case, the $\langle p_{\mathrm{T}} \rangle$ of photoproduced J/$\psi$ should increase with the centrality. Finally, combining the analyses in UPC and in peripheral collisions could help extracting the photonuclear cross section and providing new input for the study of the gluon distributions at very low Bjorken-$x$ [22].

* * *

I would like to thank the French Physical Society (SFP) and the Europhysics Letter (EPL) journal for the poster award and the opportunity of this publication.

REFERENCES


[1] Matsui T. and Satz H., *Phys. Lett. B*, **178** (1986) 416.
[2] Thews R. L., Schroedter M. and Rafelski J., *Phys. Rev. C*, **63** (2001) 054905.
[3] Braun-Munzinger P. and Stachel J., *Phys. Lett. B*, **490** (2000) 196.
[4] ALICE Collaboration (Acharya S. *et al.*), *JHEP*, **07** (2018) 160.
[5] LHCb Collaboration (Aaij R. *et al.*), *Phys. Lett. B*, **774** (2017) 159.
[6] ALICE Collaboration (Abelev B. B. *et al.*), *Phys. Lett. B*, **734** (2014) 314.
[7] ALICE Collaboration (Adam J. *et al.*), *JHEP*, **05** (2016) 179.
[8] ALICE Collaboration (Adam J. *et al.*), *Phys. Lett. B*, **766** (2017) 212.
[9] ALICE Collaboration (Adam J. *et al.*), *Phys. Rev. Lett.*, **116** (2016) 222301.
[10] Du X. and Rapp R., *Nucl. Phys. A*, **943** (2015) 147.
[11] Zha W. for the STAR Collaboration, *J. Phys. Conf. Ser.*, **779** (2017) 012039.
[12] Ivanov I. P., Nikolaev N. N. and Savin A. A., *Phys. Part. Nucl.*, **37** (2006) 1.
[13] ALICE Collaboration (Abelev B. *et al.*), *Phys. Lett. B*, **718** (2013) 1273.
[14] ALICE Collaboration (Abelev B. B. *et al.*), *Phys. Rev. Lett.*, **113** (2014) 232504.
[15] ALICE Collaboration (Acharya S. *et al.*), *Phys. Lett. B*, **798** (2019) 134926.
[16] STAR Collaboration (Abelev B. I. *et al.*), *Phys. Rev. C*, **77** (2008) 034910.
[17] PHENIX Collaboration (Afanasiev S. *et al.*), *Phys. Lett. B*, **679** (2009) 321.
[18] Baltz A. J., *Phys. Rep.*, **458** (2008) 1.
[19] Krauss F., Greiner M. and Soff G., *Prog. Part. Nucl. Phys.*, **39** (1997) 503.
[20] von Weizsacker C. F., *Z. Phys.*, **88** (1934) 612.
[21] Williams E. J., *Kong. Dan. Vid. Sel. Mat. Fys. Med.*, **13N4** (1935) 1.
[22] Contreras J. G., *Phys. Rev. C*, **96** (2017) 015203.
[23] Aamodt K. *et al.*, *JINST*, **3** (2008) S08002.
[24] ALICE Collaboration (Abelev B. B. *et al.*), *Int. J. Mod. Phys. A*, **29** (2014) 1430044.
[25] ALICE Collaboration (Acharya S. *et al.*), *Eur. Phys. J. C*, **77** (2017) 392.
[26] H1 Collaboration (Aktas A. *et al.*), *Eur. Phys. J. C*, **46** (2006) 585.
[27] ZEUS Collaboration (Chekanov S. *et al.*), *Eur. Phys. J. C*, **24** (2002) 345.
[28] Gay Ducati M. B. and Martins S., *Phys. Rev. D*, **97** (2018) 116013.
[29] Cepila J., Contreras J. G. and Krelina M., *Phys. Rev. C*, **97** (2018) 024901.